

**FINAL REPORT  
FOR  
GLAS 532nm OPTICAL DETECTOR**

*Final -  
1/11/94 - R  
023542*

**CONTRACT NAS5-32975**

**SUBMITTED BY:  
INTEVAC, INC.  
ADVANCED TECHNOLOGY DIVISION  
3550 BASSETT STREET  
SANTA CLARA, CA 95054-2704**

**KEY PERSON:  
ROSS A. LaRUE  
PROGRAM MANAGER  
PHONE: (408) 496-2872  
FAX: (408) 654-9869  
EMAIL: rlarue@intevac.com**

**Report No. ATD32975F**  
August 11, 1997  
Intevac  
Advanced Technology Division

1.0 Introduction

Quantum Efficiency at 532nm	>40%
Sensitivity	Single Photon
Pulse to Pulse Dynamic Range (5nsec pulses, 40Hz rep. rate)	$10^6$
Largest LIDAR Return Signal	$3 \times 10^8$ counts/sec.
Maximum Photon Counting Rate	$3 \times 10^8$ counts/sec.
R.F. Requirements	4-6 nsec. pulses
Detector Life	3 years 1/2 BOL
Weight	< 1Kg
Diameter	<6 cm
Length	<10 cm
Operating Temperature	-30°C-+20°C
Radiation	50 Krad total dose

Table 1.1 GLAS detector requirements. Operating temperature and radiation hardness have not yet been investigated.

The GLAS detector requirements are listed in Table 1.1. All three detectors fabricated under contract meet weight, diameter, length, r.f., and quantum efficiency requirements, although the quantum efficiency was 1-4% below the required goal. Although not measured, r.f. requirements were satisfied based on previous

measurements of similar if not identical detectors for other government programs and a detailed understanding of the physical issues involved.

Test data measured at Intevac included 532nm quantum efficiency measurements, gain and photon counting performance measurements. Two detector approaches in order to obtain the single photon sensitivity requirement were designated in the technical approach which were a high voltage Schottky diode anode approach and a lower tube voltage APD anode approach. The later approach provided the required single photon sensitivity requirement as measured by Intevac. Details of the detector measurements for tubes with serial number 00066 (high voltage approach) and 00077 (APD approach) can be found in the GLAS Interim Report. A summary of the detector measurements made at Intevac are listed in Table 1.2.

Tube (serial#)	532nm Q.E.	Gain	Single Photon Sensitivity
00066	36.2%	maximum 2,537	poor
00077	39%	maximum 15,000	excellent
00093	38%	maximum 12,000	poor

Table 1.2 A summary of Intevac test data measured on three detectors built for GLAS.

The remainder of this report is divided into three sections. Section 2.0 discusses in detail photon counting issues, in particular analysis of the required gain to obtain a high photon counting efficiency. This analysis is then used to re-investigate the data obtained for tube 00077 as reported in the GLAS Interim Report. Section 3.0 discusses the most recent test results for tube 00093. Section 4.0 discusses recent more accurate test results on an APD anode tube identically fabricated as tube 00077. This detector was built for another program but supports the conclusions reached in section 2.0. Section 5.0 concludes.

## 2.0 Counting Efficiency Issues

This section reviews counting efficiency issues, in particular, for the first tube delivered under contract which was tube 00077. Additional information for this device can be found in the GLAS Interim Report. The counting efficiency is computed as a function of tube gain. The computation agrees with the experimental result and extrapolation to higher tube gains shows that a counting efficiency of 99.6% is obtainable with a tube gain of 15,000. The gain necessary to obtain good counting efficiency is determined by the

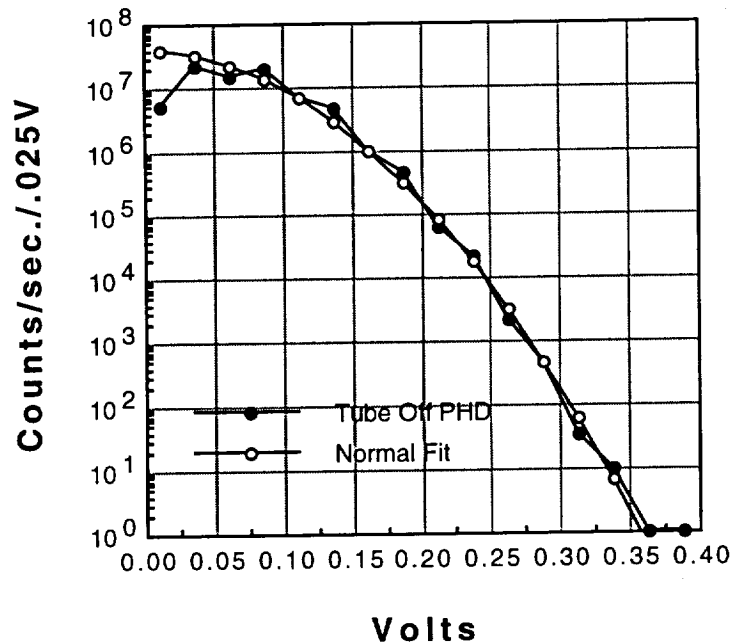


FIG. 2.0. Measured preamp system noise distribution and Gaussian fit. The APD bias was on during this measurement but the tube bias was off.

system preamp noise. A plot of the measured system preamp noise distribution is shown in FIG. 2.0. This distribution is obtained by measuring the number of counts at a particular trigger level with the tube voltage off but the APD bias on (+65V). The data is then

differentiated and a Gaussian or normal distribution fit is performed to obtain the variance. The result is (see FIG. 2.0),

$$P(V_{\text{trigger}}) = A \exp(-V_{\text{trigger}}^2 / 2\sigma^2)$$

$$A = 3.836 \times 10^7 \text{ counts/second/25mV}$$

$$\sigma^2 = \text{variance} = 3.663 \times 10^{-3} \text{ Volts}^2$$

This distribution can be used to compute the count rate and counting efficiency when the high voltage tube bias is turned on and illumination is present. The physical basis for this computation is shown in FIG. 2.1. The result is computed for a noise free tube in

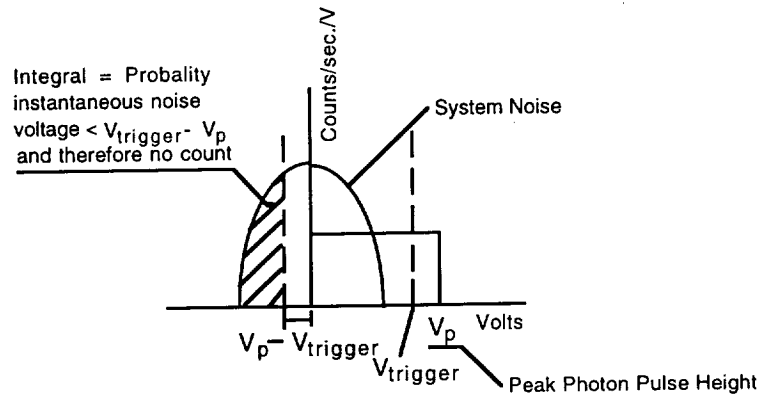


FIG. 2.1 The probability of the instantaneous preamp system noise voltage dropping below the threshold value  $V_{\text{trigger}} - V_p$  is used to compute the loss in counting efficiency. The normalized integral of the area of the Gaussian shown is equal to this probability.

which each photon results in identical charge packets out of the detector into the preamp/counter system. Less than unity counting efficiency is therefore due to insufficient gain of the single photon pulse height in which the preamp system noise affects the counting efficiency. The bandwidth of the detector and preamps greatly exceeds the counter bandwidth. Therefore, for a particular trigger

level of the counter, a photon pulse will not be counted when the instantaneous noise voltage due to the preamp drops below the threshold value  $V_{\text{trigger}} - V_p$ . The probability of this occurring for each photon is the normalized integral of the Gaussian distribution shown in FIG. 2.0 and FIG. 2.1 [1], [2]. The integration limits are from  $V_{\text{trigger}} - V_p$  to  $-\infty$ . The normalization constant is the inverse of the integral of the entire Gaussian. The count rate including system preamp noise counts is therefore,

$$\text{Counts/sec.} = (A\sigma\sqrt{\pi/2})[1 - \text{erf}(V_{\text{trigger}}/\sqrt{2}\sigma)] + (I_{\text{cath}}/q) \times$$

$$\begin{array}{ll} \eta & V_p > V_{\text{trigger}} \\ (1 - \eta) & V_p < V_{\text{trigger}} \end{array}$$

where,  $\eta$ , the counting efficiency is,

$$\eta = .5 \times \{1 + \text{erf}[|V_{\text{trigger}} - V_p|/\sqrt{2}\sigma]\}$$

This function is plotted in FIG. 2.2 along with the experimental data obtained from tube 00077. The cathode current in this case was  $2.0 \times 10^{-14}$  A at a neutral density filter of 6 and the cathode dark current (corrected for counting efficiency) was 830 counts/sec. The peak photon pulse height was taken to be .3375V as determined from the peak value of the single photon pulse height distribution. The residual discrepancy between the computed and experimental count rates in FIG. 2.2 may be due to detector or multiplication noise. The counting efficiency at a trigger level of .3V was measured to be 80.8% at the ND6 light level. The average over all light levels was 68.3%, however, the neutral density filters had not been cleaned prior to testing. The computed counting efficiency at a trigger level of .3V is 73.2% which is just slightly over the average level. Considering the accuracy of the measured values the computed count rate and counting efficiency is in good agreement with experiment.

The measured tube gain which yielded the data shown in FIG. 2.2 was only 11,000. Additional gain up to 14,000 or more was realizable by increasing the APD bias. The breakdown voltage for this anode was +71V. Since the peak pulse height,  $V_p$ , is

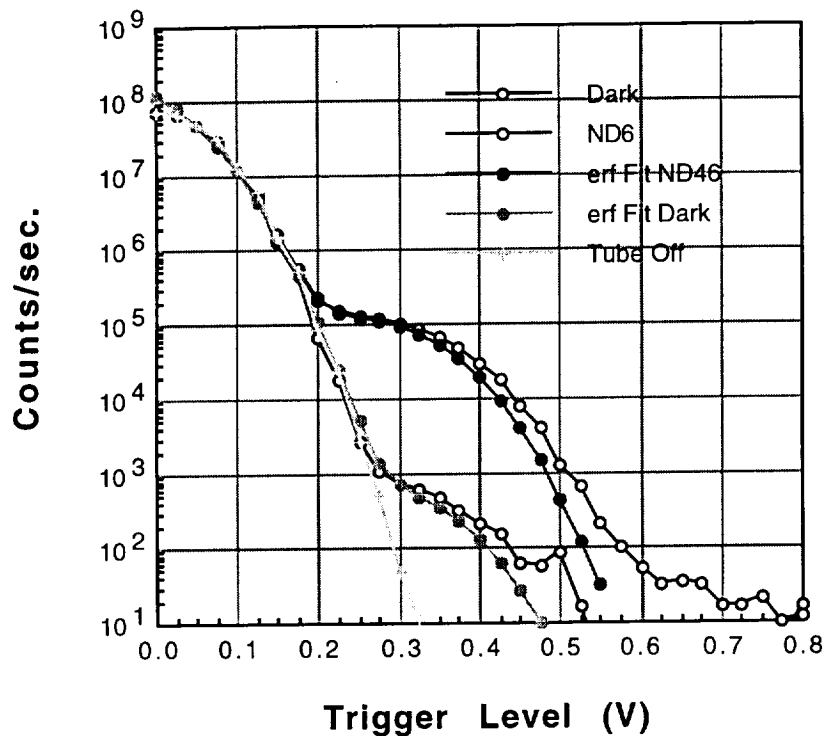


FIG. 2.2 Measured and computed count rates at a light level of neutral density filter 6 and in the dark. The measured and computed counting efficiencies at a trigger level of .3V agrees well. The preamp system noise counts at this trigger level was about 50.

proportional to tube gain, the above expression for counting efficiency can be used to compute counting efficiency versus tube gain. All other parameters are left unchanged. This result is shown in FIG. 2.3 which plots counting efficiency versus tube gain for tube 00077. This result indicates that a tube gain of 15,000 will result in a counting efficiency of 99.6%. This is due to the fact that the error function is a relatively fast function of its argument.

[1] Motchenbacher, Fitchen, Low Noise Electronic Design, John Wiley & Sons, 1973, pp. 8-9.

[2] Bennett, A. R., Electrical Noise, McGraw-Hill, New York, 1960, pp.42.

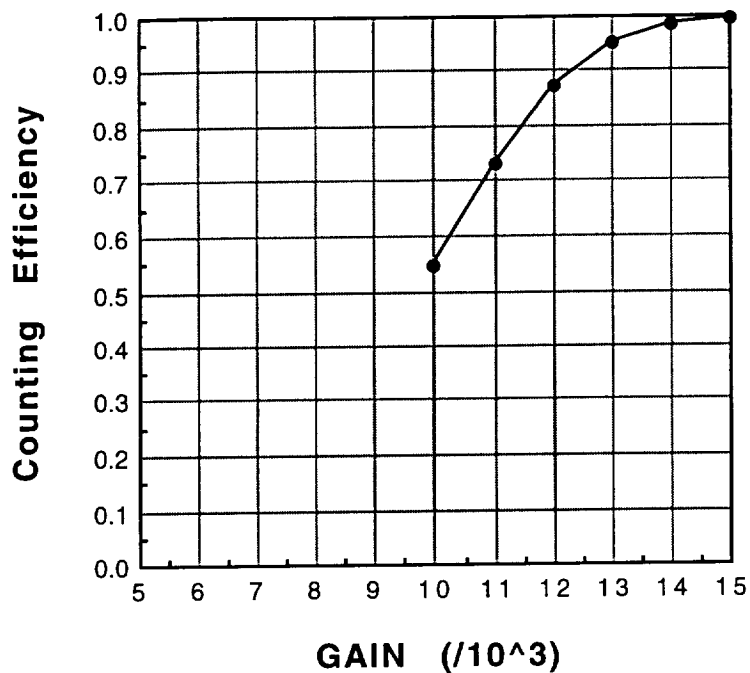


FIG. 2.3 Computed counting efficiency versus tube gain for tube 00077. Although not measured a tube gain of 15,000 results in a counting efficiency of 99.6%. The measured counting efficiency at a gain of 11,000 was 80.8%.

### 3.0 Tube (Serial #00093) Test Results

A second tube with approximately 38% quantum efficiency was fabricated and tested in order to complete the deliverables under contract. This tube was characterized for 532nm quantum efficiency, tube gain at various APD anode biases and tube voltages, and photon counting performance. FIG. 3.0 shows the measured tube gain versus tube voltage for various APD anode biases. The APD used for this tube was a thinner epitaxial device. The doped reach through layers were 1 $\mu$  below the top Schottky contact. The breakdown voltage was approximately +36V. The reach through voltage was approximately +28V which gave an 8V operating range. The reach through voltage is nominally designed for +12V. A peculiar feature of the data in FIG. 3.0 is the sag or droop in gain with tube voltage at the higher AD anode biases. Since gain is



proportional to tube voltage for all Schottky diode anode tubes fabricated at Intevac

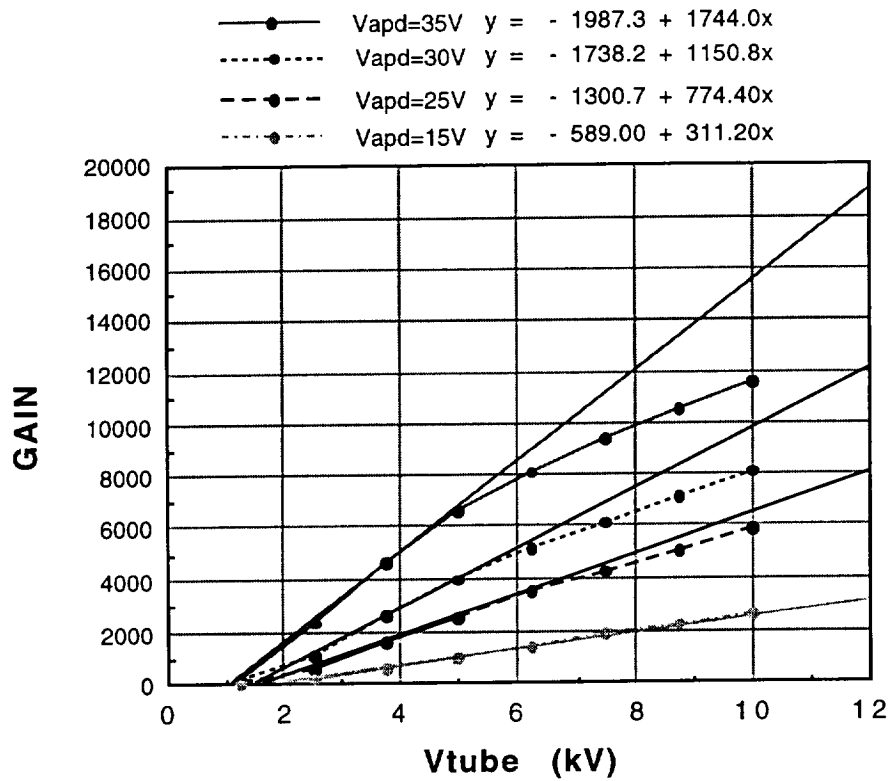


FIG. 3.0 Measured tube gain for tube 00093 versus tube voltage and APD bias.

it is expected that tubes with the Schottky AD anode should display the same linearity. However, this is not the case. The maximum gain achievable for this tube was only 12,000. Qualitatively, this same effect has been observed on other APD anode tubes but to a lesser degree. The reason for this sag is not understood, however, it is speculated that electron bombardment of the avalanching region  $1\mu$  below the surface may result in unthermalized electrons in the multiplication region which do not experience the avalanche process. In addition localized heating of the crystal per incident electron may cause the localized breakdown voltage to increase and therefore cause the gain to droop. It is further speculated at this point that a thicker undoped region between the Schottky contact and doped reach through layers will remedy this. All tubes fabricated in the

future will have an undoped  $1.5\mu$  layer as opposed to  $1\mu$  for this device and the resulting gain droop will be characterized.

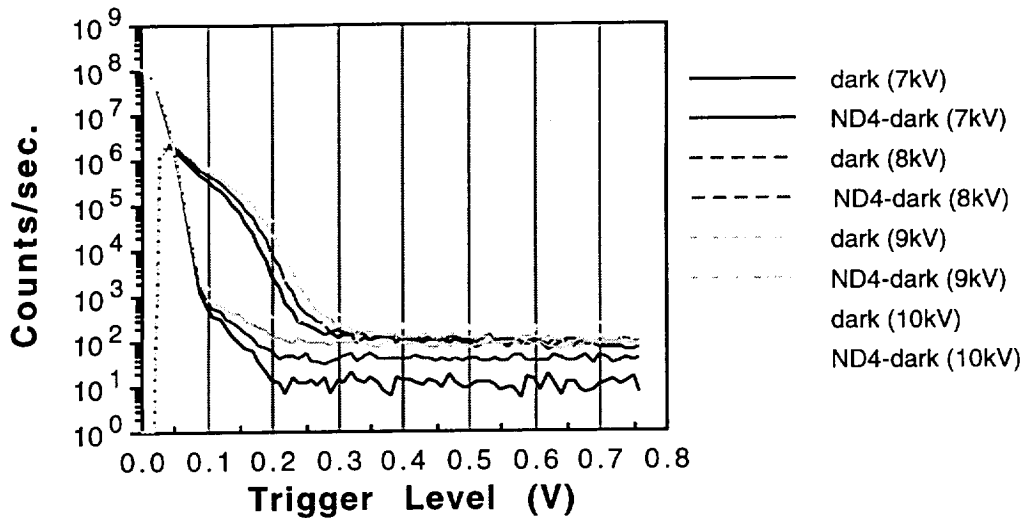


FIG. 3.1 Photon counting performance of tube 00093 at a light level corresponding to  $1.94 \times 10^6$  electrons/sec. cathode current. The droop in counting efficiency with increasing trigger level is likely related to a problem with the APD anode.

FIG. 3.1 displays the photon counting performance of tube 00093, the second deliverable tube under NASA GLAS contract. The figure shows the counting performance at tube voltages of 7kV, 8kV, 9kV and 10kV. The APD bias was at or slightly below the breakdown voltage of +35V. Measurements were taken in the dark and at an ND4 light level of 0.31pA cathode current which corresponds to  $1.94 \times 10^6$  photoelectrons/sec. The dark count rate was subtracted from the count rate with illumination for the four tube biases shown. The peak count rate at a tube bias of 10kV was  $2.47 \times 10^6$  counts/sec. and occurs at a trigger level where the dark counts are comparable in magnitude. The count rate then rapidly sags or decreases with increasing trigger level. The reason for this poor performance is unknown but it is speculated that gain non-uniformities in the APD anode could account for the low photon counting efficiency. Alternatively, as mentioned previously, electron bombardment of the avalanche region which was only  $1\mu$  below the anode surface may result in poor single photoelectron pulse height statistics. In any

case this tube failed to meet NASA GLAS contract requirements and is therefore classified as scrap.

#### 4.0 More Recent Results

A third tube, 6D230, was characterized in detail for counting efficiency. These results are shown in FIG. 4.0 in which the count rate was characterized at 7.5kV, 8.5kV and 9.5kV tube operating voltage. The APD avalanche region was  $1.5\mu$  below the top Schottky contact. The APD bias was +50V, approximately 2V below breakdown. The cathode current at a neutral density filter of 6.0 was measured to be 27.6fA. This was accomplished by using two neutral density filters, ND 2.0 and ND 4.0. The cathode current using an ND 2.0 filter was measured with a picoammeter to be .280nA. A calibrated ND 4.0 filter was then inserted in series with the ND 2.0 filter. The

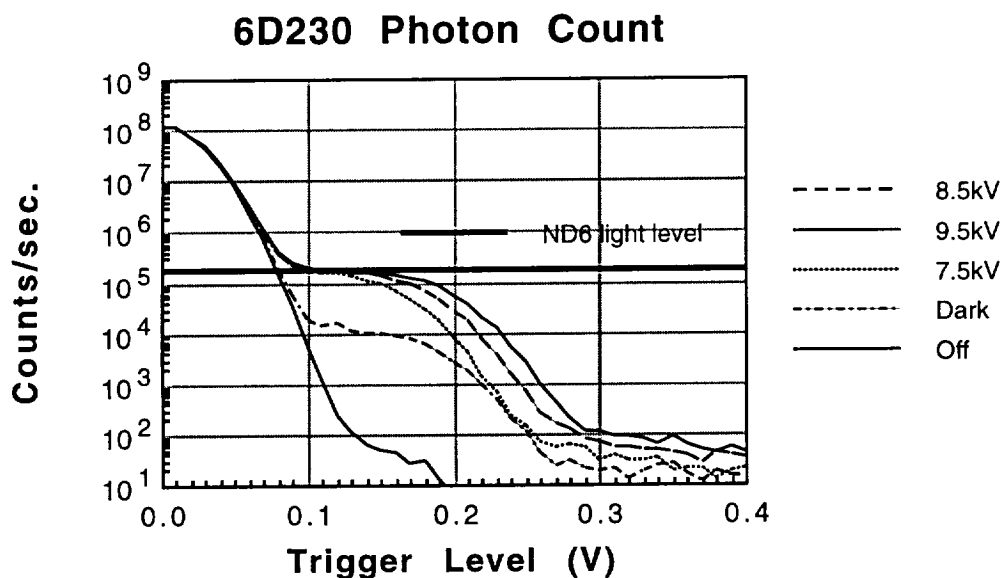


FIG.4.0 Measured count rate of tube 6D230 at 7.5kV, 8.5kV and 9.5kV tube bias with a cathode current of 27.6fA. The dark count rate and preamp noise count rate with tube bias off is also shown. The counting efficiency at the higher tube bias was in excess of 90%.

calibration of the ND 4.0 filter was accomplished by using a laser at the same tube test wavelength and observing the decrease in a silicon photocell current when the ND 4.0 filter was inserted in

series with the ND 2.0 filter. The average decrease in photocell current was measured to be  $.984 \times 10^{-4} \pm .005 \times 10^{-4}$ . The electron flux from the cathode at a neutral density factor of 6.0 was therefore  $1.72 \times 10^5$  electrons/sec. This value is plotted in FIG. 4.0 by the bold line. The three count traces at 7.5kV, 8.5kV and 9.5kV with ND6 illumination are also shown. At a trigger level of .14V. The counting efficiency well exceeds 90%. There is also steady improvement of counting efficiency with tube bias and increasing gain. The noise system counts and cathode dark counts are also shown in this figure. The cathode dark count was approximately 9,936 electrons/sec. The cathode diameter for this tube was 8mm.

Lastly, the measured and computed counting efficiency at a

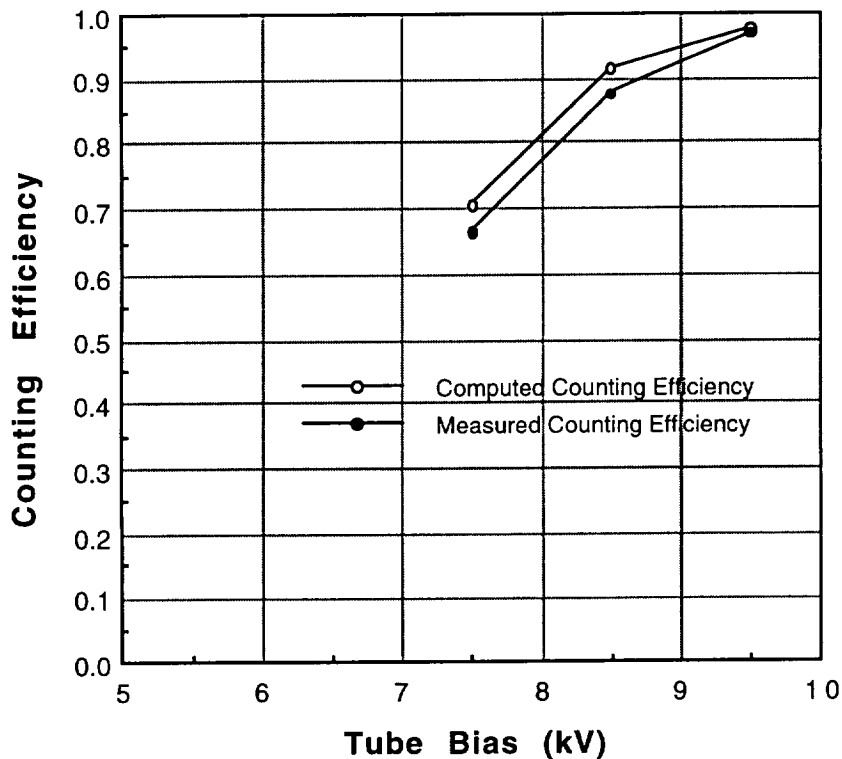


FIG. 4.1 Measured and computed counting efficiencies for tube 6D230 versus tube bias. The computed values are based on the formula derived in section 2.0.

trigger level of .14V is plotted in FIG. 4.1. The computed values are obtained by using the formula for counting efficiency derived in section 2.0. In using this formula the system noise variance,  $\sigma^2$ , was

obtained by fitting the derivative of the tube off trace in FIG. 4.0 to a Gaussian distribution as described in section 2.0. The peak photon pulse height,  $V_p$ , was obtained for each tube bias by noting that according to the counting efficiency formula the counting efficiency is 50% when the trigger voltage equals  $V_p$ . These values also coincide with the peak value of the pulse height distribution obtained by differentiating the data in FIG. 4.0. To within experimental accuracy the measured and computed counting efficiencies agree well. The tube gain at 9.5kV tube bias was measured to be approximately 12,000-13,000. A more careful determination of the gain was not possible due to a testing error during demonstration purposes for another program for which the tube was fabricated. The tube had arced and the anode was damaged.

## 5.0 Conclusion

The analysis and data presented in sections 2.0 and 4.0 conclusively shows that a detector gain of 15,000 is sufficient to obtain near 100% counting efficiency. The formula for counting efficiency derived in section 2.0 usefully connects detector gain requirements with the limitations imposed by system preamp noise for high counting efficiency. The test data shown in section 4.0 is the first careful determination of counting efficiency as measured at Intevac. It should be reiterated that the required detector gain for high counting efficiency is determined by the system preamp noise and is therefore likely to be user dependent. While the Intevac photon counting system uses quality preamps and a quality bias tee as described in the GLAS Interim Report these items are commercially available components. The noise figure specification of the Sonoma 310 preamp is 1.8 dB and is certainly a quality preamp but is not state of the art. From the point of view of detector robustness and user ease a detector gain of 20,000 would provide a larger trigger voltage range for 100% counting efficiency. The APD anode would not have to be biased so closely to the breakdown voltage to obtain the test results in sections 2.0 and 4.0. Also more system preamp noise could be tolerated and therefore cheaper preamps could be used. For these reasons any future technical development of the APD anode at Intevac will include improving the APD gain to a nominal value of 20. The principle

method for achieving this level of performance has recently been determined to be an increase in the doping level of any reach through layers within the diode. This is indicated in FIG. 5.0 which simulates achievable gain versus doping concentration. To what

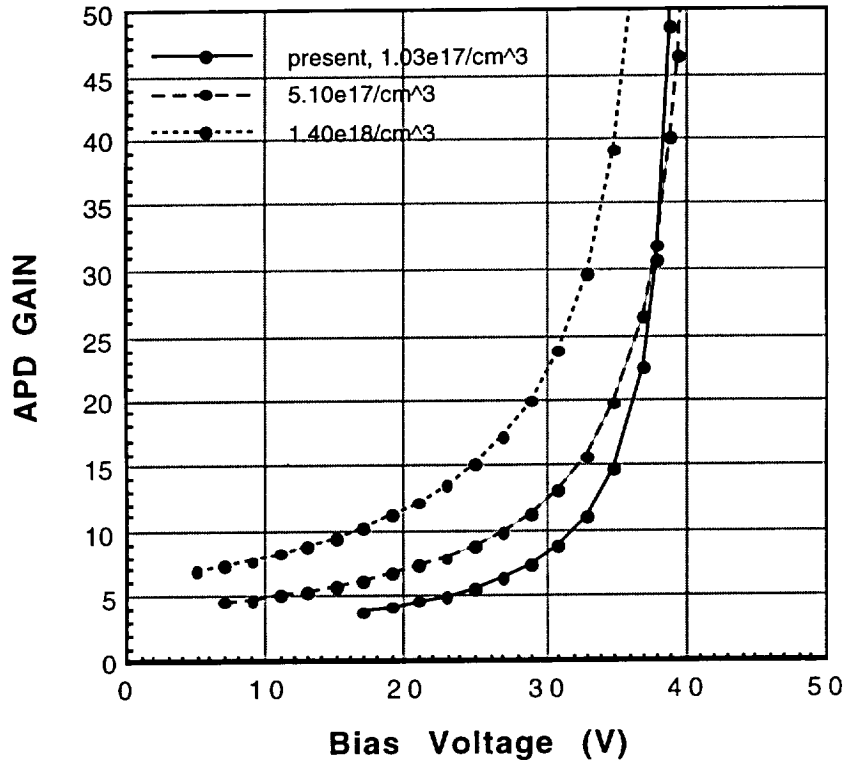


FIG. 5.0 Simulated APD gain for various doping levels of the reach through layers. The present APD structure with the lowest gain is doped approximately  $1 \times 10^{17} \text{ cm}^{-3}$  and is indicated by the solid curve.

extent the doping may be increased without other detrimental effects on APD performance is at present unknown.

REPORT DOCUMENTATION PAGE			Form Approved OMB No. 0704-0188	
Public reporting burden for this collection of information is estimated to average 1 hour per response, including the time for reviewing instructions, searching existing data sources, gathering and maintaining the data needed, and completing and reviewing the collection of information. Send comments regarding this burden estimate or any other aspect of this collection of information, including suggestions for reducing this burden, to Washington Headquarters Services, Directorate for Information Operations and Reports, 1215 Jefferson Davis Highway, Suite 1204, Arlington, VA 22202-4302, and to the Office of Management and Budget, Paperwork Reduction Project (0704-0188), Washington, DC 20503.				
1. AGENCY USE ONLY (Leave blank)		2. REPORT DATE August 1997		3. REPORT TYPE AND DATES COVERED Contractor Report
4. TITLE AND SUBTITLE 532 nm Optical Detector (Final April 2, 1996-June 30, 1997)			5. FUNDING NUMBERS  NAS5-32975	
6. AUTHOR(S)  Ross A. LaRue				
7. PERFORMING ORGANIZATION NAME(S) AND ADDRESS (ES) Intevac, Inc. Advanced Technology Division 3550 Bassett Street Santa Clara, CA 95054			8. PERFORMING ORGANIZATION REPORT NUMBER  ATD32975F	
9. SPONSORING / MONITORING AGENCY NAME(S) AND ADDRESS (ES)  National Aeronautics and Space Administration Washington, DC 20546-0001			10. SPONSORING / MONITORING AGENCY REPORT NUMBER  CR-203880	
11. SUPPLEMENTARY NOTES				
12a. DISTRIBUTION / AVAILABILITY STATEMENT Unclassified - Unlimited Subject Category: 74 Report available from the NASA Center for AeroSpace Information, 800 Elkridge Landing Road, Linthicum Heights, MD 21090; (301) 621-0390.			12b. DISTRIBUTION CODE	
13. ABSTRACT (Maximum 200 words) This report documents fabrication and testing of 532nm optical detectors. Testing and procedures included 532nm quantum efficiency, detector gain, and photon counting performance, in particular, photon counting efficiency. 532nm quantum efficiency was measured to be 36% to 39% for the detectors fabricated. Detectors with a GaAs APD anode had measured gains of 12,000 to 15,000 maximum. Photon counting efficiency for the detector with and APD anode was measured to be approximately 80% with a detector gain of 11,000. Measurements made on an identical detector, not fabricated under this contract, had a photon counting efficiency exceeding 90% with a gain of 13,000. A formula noise is derived in which the photon counting efficiency is determined by the system preamp noise and the peak single photon pulse height which is proportional to detector gain. This formula agrees well with the measured results and indicates that a detector gain of 15,000 is sufficient to provide a counting efficiency of 99.6%.				
14. SUBJECT TERMS 532nm optical detector, photon counting efficiency, GaAsP Photocathode			15. NUMBER OF PAGES 13	
			16. PRICE CODE	
17. SECURITY CLASSIFICATION OF REPORT Unclassified	18. SECURITY CLASSIFICATION OF THIS PAGE Unclassified	19. SECURITY CLASSIFICATION OF ABSTRACT Unclassified	20. LIMITATION OF ABSTRACT  UL	